Proceedings of the
Annual Stability Conference
Structural Stability Research Council
San Antonio, Texas, March 19-22, 2024

Revisiting the minimum I-section cross-sectional proportions to ensure adequate shear capacity

Namita Nayak [1], Lakshmi Subramanian [2]

Abstract

This paper discusses the conventional assumption of simply-supported boundary conditions in estimating an I-girder web's elastic shear buckling stress. Some past literature discuss an increase in the elastic buckling stress while considering the restraint from the flanges. However, few have examined the lack of adequate support at the web boundaries shared with flanges and stiffeners. This paper shows that intermediate transfer stiffeners that satisfy the minimum rigidity criteria prescribed in design codes provide adequate restraint to achieve stresses corresponding to the simply-supported edge conditions. However, at stiffener locations not coinciding with lateral or torsional restraints, there are excessive deformations at these web edges despite satisfying the minimum rigidity criteria. Similarly, the paper shows that narrow flanges in long web panels allow excessive deformations at the web-flange junctions, resulting in premature elastic shear buckling, and do not help achieve even simply-supported boundary conditions, thereby making such simplistic assumptions in design codes unsafe. This inadequate restraint, gauged by the large displacement at stiffener locations and the web-flange junctions, further exacerbates the postbuckling behavior of such girders. The paper identifies the flange and stiffener dimensions that dictate the restraint levels at the web boundaries adjoining the flanges and the stiffeners. A brief discussion of the impact of these considerations on the ultimate strength of girders is also presented using finite element simulations.

1. Introduction

The ultimate design shear capacity is usually expressed as a sum of the elastic shear buckling capacity and the postbuckling capacity. Most design specifications (EN 1993-1-5 2006; AASHTO 2020; AISC 2022) compute the elastic shear stress of an I-girder by assuming the web to be a simply-supported plate. However, different postbuckling theories form the basis of different postbuckling capacity equations. For instance, the Eurocode (EN 1993-1-5 2006) incorporates the rotated stress field theory (Höglund 1971, 1997), whereas the American codes (AASHTO 2020; AISC 2022) are primarily based on Basler's tension field theory (Basler 1961). However, all these design assumptions rely on the flanges and stiffeners providing sufficient restraint, resulting in near-zero out-of-plane deflections at the web-flange and web-stiffener boundaries. Furthermore,

[1] Ph.D. Student, Indian Institute of Technology Madras, <namitanayak519@gmail.com>
[2] Assistant Professor, Indian Institute of Technology Madras, <lakshmipriya@iitm.ac.in >

the increasing use of narrow flanges in I-sections, and greater transverse stiffener spacing, causing larger unstiffened lengths, leads to increased instability in the structure and may not meet the assumptions underlying the development of design provisions for shear buckling of I-girders.

Timoshenko (1936) initially recognized that insufficient rigidity in stiffeners leads to out-of-plane bending, causing shear buckling waves to propagate across the stiffeners. However, ensuring sufficient stiffener rigidity can diminish this bending effect, enabling the plate segment between the stiffeners to behave as if it were simply-supported. Timoshenko subsequently determined limiting values for stiffener rigidity based on various web panel aspect ratios derived from the energy method, as listed in Table 1.

Table 1: Limiting value of stiffener moment of inertia to ensure a simply-supported boundary condition for a plate having two transverse stiffeners (Timoshenko 1936)

a/h	0.400	0.500	0.667	0.833	1.000
$\gamma_{\min}$[1]	67.80	32.10	10.60	4.11	1.92

1. $\gamma_{\min} = \dfrac{12\left(1-\nu^2\right) I_{\min}}{t^3 a}$

Stein and Fralich (1949) argued that the solutions derived by Timoshenko (1936) were flawed owing to the restricted number of terms employed in representing the deformation function. Using the Lagrangian multiplier method, the authors determined the elastic shear buckling strength of infinitely long plates with evenly spaced transverse stiffeners. Subsequently, Bleich (1952) utilized the findings from Stein and Fralich (1949) and established the elastic shear buckling coefficient as a function of the panel aspect ratio and stiffener spacing. Using the elastic shear buckling strength proposed by Bleich (1952), Ziemian (2010) derived the minimum moment of inertia of the transverse stiffener given in Eq. 1.

$$I_{\min,s} = 2.5ht_w^3\left(\frac{1}{\left(a/h\right)} - 0.7\left(\frac{a}{h}\right)\right) \quad \text{for } a/h \le 1 \tag{1}$$

where $I_{\min,s}$ is the minimum moment of inertia of transverse stiffener, a is the length of web plate, h is the height of the plate, and t_w is the thickness of the web plate.

The design specifications (AASHTO 2020; AISC 2022) use Eq. 1 with the coefficient of a/h taken as 0.8 rather than 0.7 in the parentheses. Lee et al. (2003) conducted both experimental and numerical simulations and concluded that the flexural rigidity of the transverse stiffeners should be taken as six times the recommended value given in design standards (AASHTO 2020; AISC 2022) in order to resist the bending action that occurs during post buckling. However, Kim (2004) suggested that the minimum transverse stiffener rigidity proposed by Lee et al. (2003) needs to account for the greater demand on webs with larger web slenderness ratios. Consequently, based on the work by Kim (2004), the transverse stiffener requirements in both AASHTO (2020) and AISC (2022) were updated as shown in Eq. 2.

$$I_{\min,s} = \min\left(a,h\right)\times t_w^3\left[2.5\left(\frac{h}{a}\right)^2 - 2\right] \ge 0.5\times\min\left(a,h\right)\times t_w^3 \tag{2}$$

The Eurocode (EN 1993-1-5 2006) places a greater demand on the moment of inertia of intermediate transverse stiffeners than the American codes.

While some past studies examined the boundary conditions at transverse stiffener locations and the restrictions on the dimensions of transverse stiffeners incorporated in design codes, the literature on the influence of the flange plates on the I-girder webs (Al-azzawi et al. 2015; Lapira et al. 2023; Lee et al. 1996) primarily focus on accounting for the increase in the elastic shear buckling stresses of I-girder webs due to the flanges. Only a few studies (Pham and Hancock 2009; Nayak et al. 2021) have demonstrated significant flange displacement at the web-flange junctions of channel sections and I-sections. Nevertheless, there is a need for practical recommendations to address this issue. AASHTO (2020) permits I-sections with web depth-to-flange width ratios ≥ 6.0 and flange-to-web thickness ratios ≥ 1.1, anticipating that I-sections with flange dimensions satisfying these criteria exhibit behavior akin to stiffened panels when subjected to pure shear.

This paper first shows that although the minimum moment of inertia specified for the transverse stiffener in American codes (AASHTO 2020; AISC 2022) yields a minimum elastic shear buckling stress of that of simply-supported plates, achieving reasonably low out-of-plane deflections at the stiffener locations remains challenging. The paper then focuses on stiffened plates, where significantly lower elastic shear buckling stresses than simply-supported plates are observed due to excessive displacements at the web-flange junctions. Using finite element (FE) simulations, additional dimension limits are proposed to reduce the out-of-plane displacements at web boundaries. Finally, the recommended limits are demonstrated to effectively diminish the excessive deflections and enhance the ultimate shear strengths of I-girders through full nonlinear analyses.

2. Finite element modeling

The results presented in this paper are obtained from FE simulations in (ABAQUS 2022). The webs, flanges, and transverse stiffeners are modeled with general-purpose S4R shell elements. The study primarily focuses on the shear buckling of I-girder webs, and thus, the girders are subjected to pure shear loading in the FE simulations. The webs are discretized into 40 elements along their depth, with an aspect ratio of approximately one, while the transverse stiffeners and the flanges are discretized into 12 elements along their widths. In the stiffened plates, the bottom web-stiffener junction nodes at either end are modeled as hinge and roller, and the out-of-plane displacements of the two parallel unstiffened edges are constrained. Similarly, in the case of unstiffened I-girders, the bottom web-flange junction nodes at the two ends are modeled as hinge and roller, while the out-of-plane displacements are restrained along the parallel unstiffened edges.

The findings presented in Section 3 are results from eigenvalue analyses conducted using subspace iteration. The nonlinear analyses presented in Section 4 are performed using the modified Riks method by introducing an initial web out-of-flatness with a maximum magnitude of $h/10{,}000$ (to discuss behavior with near-zero imperfections) applied in the same direction as their governing eigenmodes. The Young's modulus of elasticity (E) is taken as 200,000 MPa, and the steel yield strength (f_y) is 350 MPa. The material model used in the nonlinear analyses, adopted from (Subramanian and White 2017a, 2017b), assumes a small tangent stiffness, $E/1000$, within the yield plateau (the strain reaches ten times the yield strain), followed by a strain-hardening modulus

of $E/50$. Residual stresses do not affect the shear strengths of I-sections (Nayak and Subramanian 2023) and are not used in the models presented here.

3. Influence of transverse stiffeners and flanges on the boundary condition of I-girder webs in elastic shear buckling

This section presents the results of elastic shear buckling of stiffened plates (i.e., web plates supported by transverse stiffeners) and unstiffened I-girders (i.e., web plates supported by flanges). The cross-sectional parameters used in the elastic shear buckling FE simulations are presented in Table 2. The web length, width, and thickness are denoted by a, h, and t_w, respectively. The widths and thicknesses of the transverse stiffener and flange are denoted by b_s, t_s, and b_f, t_f, respectively. The stiffeners and flanges in these studies satisfy the minimum moment of inertia of transverse stiffeners (Eq. 6.10.11.1.3-1 in AASHTO (2020)) and minimum flange width and thickness recommended in AASHTO (2020) (Eq. 6.10.2.2-2 and Eq. 6.10.2.2-3).

Table 2: List of cross-sectional parameters used in finite element simulations.

Cross-sectional parameter	Stiffened plates	Unstiffened I-girders
No of models	632	882
a/h	0.5-1.0	1.0-3.0
h/t_w	70-300	70-300
h/b_s	6.0-16.0	-
t_s/t_w	0.73-6.25	-
h/b_f	-	4.0-6.0
t_f/t_w	-	1.1-4.0

This section first examines the influence of transverse stiffeners on the web boundary condition. Subsequently, the boundary condition at the junction of the web and flange is analyzed, considering the addition of flange plates to the webs, and assessing the out-of-plane deflections at the web panel boundaries.

3.1. Impact of transverse stiffeners on out-of-plane displacement at the web boundaries

The studies in this section focus on the buckling of stiffened plates subjected to pure shear. The out-of-plane deflections at the web-stiffener junctions are examined by ensuring that the moment of inertia of transverse stiffeners is at least $I_{\min,s}$.

Figs. 1(a) - 1(e) show representative buckling modes of the transversely stiffened plates. Figs. 1(a) - 1(c) show the buckling modes of web aspect ratios (a/h) of 0.5, 0.75, and 1.0 for webs of slenderness 100, web depth to stiffener width of seven, and t_s/t_w of 1.8. Figs. 1(d) and 1(e) present the buckling modes for an aspect ratio of 0.5, but with increased transverse stiffener dimensions in Fig.1(d) ($h/b_s = 6$, $t_s/t_w = 2.1$) and increased web slenderness of 150 in Fig. 1(e). The ratio of the maximum out-of-plane displacement of the web-stiffener junction to that of the web is denoted by u_s/u_w.

Figs. 1(a) - 1(e) corroborate the expected behavior of stiffened plates, such as:

1. Figs. 1(a) - 1(c) show that for given transverse stiffener and web dimensions, the maximum out-of-plane displacements at the stiffener edges are observed for the stiffened plate with the smallest web aspect ratio of 0.5 (u_s/u_w = 0.24).

2. By comparing Figs. 1(d) and 1(a), it is observed that increasing the transverse stiffener dimensions is effective in reducing the out-of-plane displacement at the web boundaries and thus increases the elastic shear buckling stress (τ_{cr}).

3. Fig. 1(e) shows that the out-of-plane displacements at the web-stiffener edge are nearly zero, indicating that a larger web slenderness places a smaller demand on the transverse stiffeners to control deflections at the relatively low values of elastic buckling stress. In comparing Figs. 1(a) and 1(e), it is evident that, for a given stiffener dimension, the ratio of elastic shear buckling stress of the stiffened plate to that of the simply-supported plate ($\tau_{cr}/\ \tau_{crSS}$) is larger for the relatively slender web.

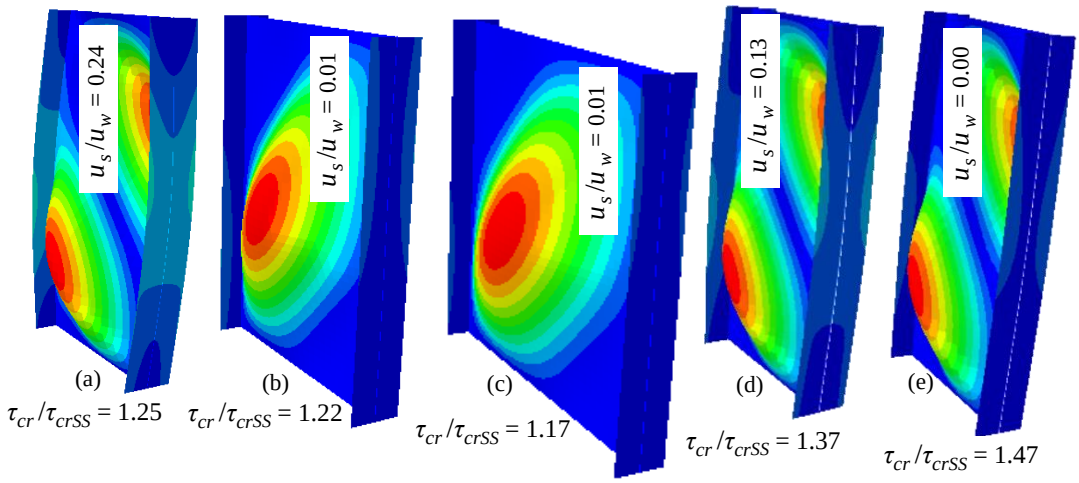

Figure 1: Elastic shear buckling modes of stiffened plates (a) a/h = 0.5, h/t_w =100, h/b_s = 7, t_s/t_w = 1.8 (b) a/h = 0.75, h/t_w = 100, h/b_s = 7, t_s/t_w = 1 8 (c) a/h = 1.0, h/t_w = 100, h/b_s = 7, t_s/t_w = 1.8 (d) a/h = 0.5, h/t_w = 100, h/b_s = 6, t_s/t_w = 2.1 (e) a/h = 0.5, h/t_w = 150, h/b_s = 7, t_s/t_w = 1.8

The studies show that both the width and thickness of transverse stiffeners substantially impact the out-of-plane deflections at the web-stiffener junctions. To illustrate the impact of transverse stiffener dimensions on the out-of-plane displacements at the web boundaries, the moment of inertia of the transverse stiffener about its major axis (i.e., the axis normal to the deflection component considered in the studies in Eq. 3) is considered as the primary variable. Fig. 2 plots the relative out-of-plane displacement at the web-stiffener junction (u_s/u_w) against $I_s/I_{min,s}$, where I_s represents the moment of inertia of the transverse stiffener calculated using Eq. 3. The displacements are shown for the transverse stiffeners which satisfy $I_s/I_{min,s} \geq 1.0$.

$$I_s = \frac{b_s t_s^3}{12} \tag{3}$$

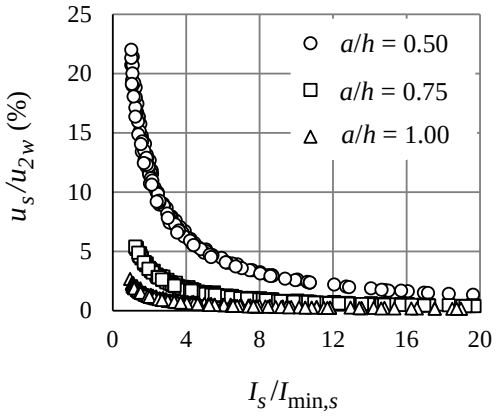

Figure 2: Variation of the out-of-plane displacements at the web-stiffener junctions for stiffened plates with the transverse stiffener moment of inertia

The following conclusions are drawn from Fig. 2:

1. This plot demonstrates that the transverse stiffeners with moments of inertia approximately $I_{\min,s}$ resulted in deflections at web boundaries, which are more than 20% of that of the web.

2. For a given $I_s/I_{\min,s}$, the relative deflections at the web-stiffener junction and the web reduce with increasing panel aspect ratio. However, for the stiffened plates with a web aspect ratio equal to one, the deflections are more considerable compared to the stiffened plates with a/h = 0.75 for a given $I_s/I_{\min,s}$. This is due to the smaller magnitude of $I_{\min,s}$ used in AASHTO (2020) for $a/h \geq 1.0$. Thus, for a given value of $I_s/I_{\min,s}$, the moment of inertia of stiffener for a stiffened panel with a/h of one is less than that of a panel with a/h of 0.75, resulting in a smaller deflection increase.

3. This figure shows that deflections decrease drastically with an increase in $I_s/I_{\min,s}$ before reaching a plateau. This illustrates that I_s, calculated as per Eq. 3, is a key variable in determining the web plate behavior when subjected to pure shear.

4. It is evident that using transverse stiffeners with $\boldsymbol{I_s \geq 2\ I_{min,s}}$ restricts the out-of-plane deflections at the web-transverse stiffener locations to less than 10% of the maximum web out-of-plane deflection for $a/h \geq 0.5$.

3.2 Impact of flanges on out-of-plane displacements at the web boundaries

This section presents elastic buckling FE simulations that examine the effect of flanges on the elastic shear buckling of web plates. Similar to the stiffened plates, the unstiffened I-girders are modeled with two unstiffened, simply-supported parallel edges. The elastic shear buckling modes of the unstiffened I-girders are presented in Fig. 4, where the aspect ratio a/h is varied, keeping the other parameters such as the web slenderness ratio and the flange dimensions constant (h/t_w = 70, h/b_f = 6, and t_f/t_w =1.1).

The following conclusions are drawn from Figs. 4(a)-4(d):

1. The unstiffened I-girder with a/h = 1.0 has the least out-of-plane deflection at the web-flange junction (~2% of the maximum web out-of-plane displacement).

2. The relative out-of-plane displacement at the web-flange junction (u_f/u_w) increases with an increase in the aspect ratio of the web. The out-of-plane deflection at the web-flange junction (u_f) is nearly equal to the maximum web deflection (u_w) for the unstiffened I-girder with the largest aspect ratio (a/h = 3.0), or the largest supported edge of the web for a constant web depth.

3. It is also observed that the ratios of elastic shear buckling stresses of the unstiffened I-girders (τ_{cr}) to those of the simply-supported plates (τ_{crSS}) reduce with increasing aspect ratios, reaching a minimum τ_{cr}/τ_{crSS} as low as 0.57 for a/h of 3.0. This increasing instability is triggered by the increasing out-of-plane deflections at the flange-web boundaries.

It is evident that using narrow flanges results in significant out-of-plane displacements at the web boundaries. Therefore, the I-girder webs fail to behave as simply-supported plates. The significant deflection also results in shear buckling stresses smaller than those of simply-supported plates. This requires introducing an additional limiting parameter to prevent using flexible flanges, distinct from the flange width and thickness, to control excessive deflections.

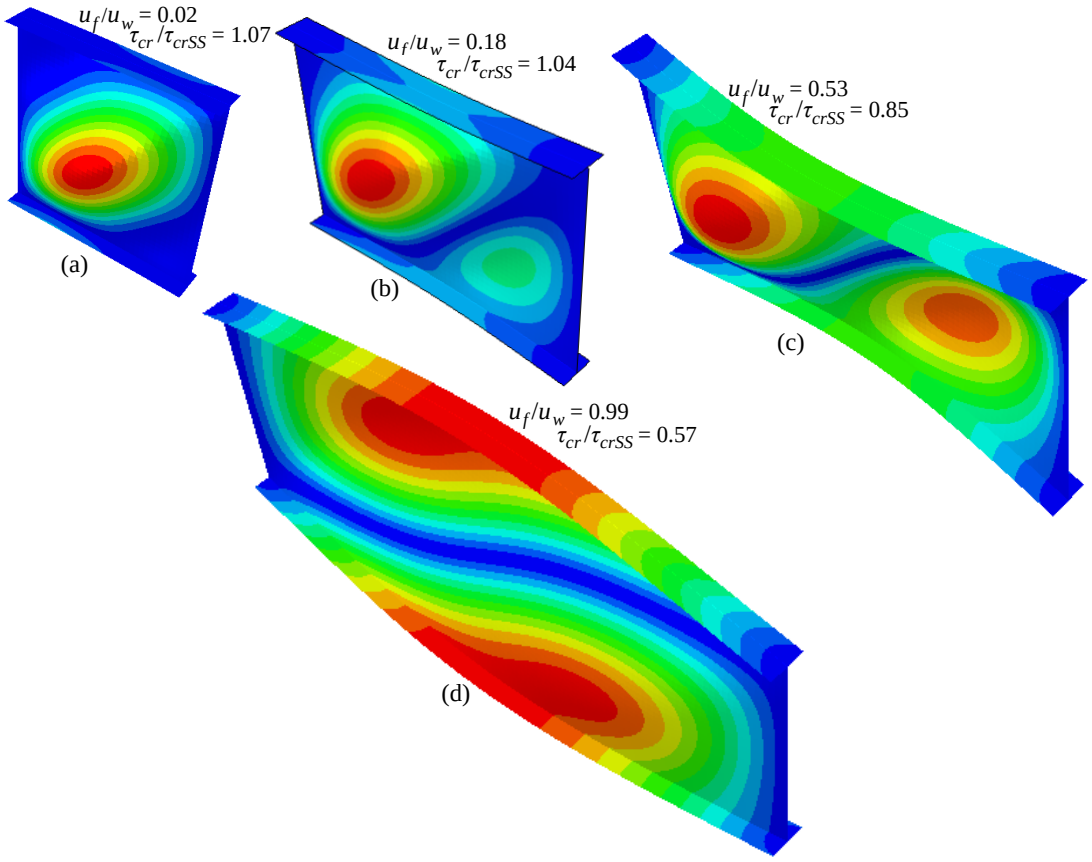

Figure 3: Eigen buckling modes of unstiffened I-girders with h/t_w = 70, h/b_f = 6.0, t_f/t_w = 1.1 (a) a/h = 1.0, (a) a/h = 1.5, (a) a/h = 2.0, (a) a/h = 3.0

As observed with the stiffened plates, the increased flange dimensions and increased web slenderness cause reduced deflections at the web-flange junctions. Section 3.1 established that the stiffeners' major axes moments of inertia control the out-of-plane deflection at the web boundaries. While the in-plane flange rigidity or its torsional rigidity is expected to provide the restraint to the

web, the out-of-plane flange moment of inertia (calculated using Eq. 4) is observed to govern the web plate behavior where excessive out-of-plane displacements are observed. Similar to the transverse stiffener moment of inertia requirements given in Eq. 2, a minimum flange moment of inertia is defined in this paper ($I_{\min,f}$) in Eq. 5 for web aspect ratios (a/h) greater than one. Eq. 5 is derived by inverting the panel length and height terms for transverse stiffeners in Eq. 2. Eq. 5 is similar to the minimum moment of inertia requirement for longitudinal stiffeners recommended in Eq. 6.10.11.3.3-1 in AASHTO (2020).

$$I_f = \frac{b_f t_f^3}{12} \tag{4}$$

$$I_{\min,f} = h t_w^3 \left[2.5 \left(\frac{a}{h} \right)^2 - 2 \right] \geq 0.5 h t_w^3 \tag{5}$$

Studies show that u_f exceeds 10% of u_w for webs with $a/h \geq 1.5$, with more significant displacements in larger unstiffened panels. Hence, Fig. 6 shows the variation in the web out-of-plane deflections with $I_f/I_{\min,f}$ for the unstiffened I-girders with $a/h \geq 1.5$. The relative flange and web out-of-plane displacements (u_f/u_w) decrease with an increase in $I_f/I_{\min,f}$, exhibiting a behavior identical to that of transversely stiffened plates discussed in Section 3.1. From this plot, it can be observed that, for the I-girders with $I_f/I_{\min,f} \geq 2$, the flange out-of-plane deformation is less than 10% of u_w. The relative flange displacement of 10% is acceptable, given that the elastic shear buckling coefficients for such girders are greater than those of simply-supported plates. Therefore, the authors suggest using flange dimensions that meet the condition $I_f \geq 2I_{\min,f}$.

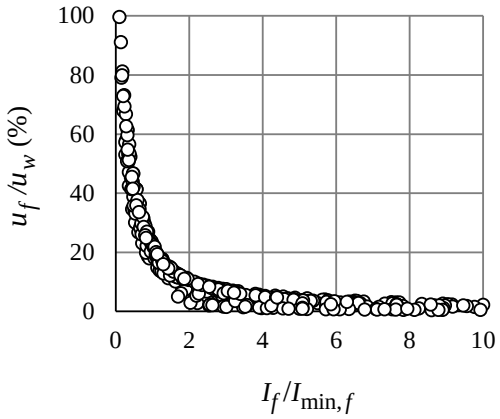

Figure 4: Out-of-plane displacement at the web-flange junction for unstiffened I-girders plotted with the moment of inertia of the flange plates

4. Nonlinear finite element analysis of unstiffened I-girders subjected to pure shear

This section presents the results from geometric and material nonlinear FE analyses for unstiffened I-girders subjected to pure shear. These are conducted with near-zero imperfections and no residual stresses, as discussed in Section 2. These studies are presented to draw parallels between the modal displacements discussed earlier and the displacements from nonlinear analyses. The elastic buckling analyses showed that the out-of-plane displacements are more pronounced in larger panel

aspect ratios ($a/h \geq 1.5$) and for stockier webs. Hence, six case studies are examined here, with aspect ratios ranging from 1.5 to 4.0, and web slenderness ratios of 100 and 150. Each case study analyzes two girders, differing in their flange dimensions. The cross-sectional dimensions of the twelve unstiffened I-girders are listed in Table 3. The depth of the girders is 2000 mm. The unstiffened I-girders in the table are labeled as UG*x*-*y*, where *x* denotes the case study number from 1 to 6, and $y = 1$ is assigned to the smaller flange dimensions with $I_f / I_{\min,f} < 2$, and $y = 2$ to the larger flange dimensions with $I_f / I_{\min,f} \geq 2$. All flanges satisfy other requirements specified in AASHTO (2020).

Table 3: Dimensions of the unstiffened girders

Case study	Specimen	a/h	h/t_w	$I_f / I_{min,\,f}$ $(b_f \times t_f)$ mm^2	Specimen	a/h	h/t_w	$I_f / I_{min,\,f}$ $(b_f \times t_f)$ mm^2
1	UG1-1	1.5	100	1.6 (333.3× 30.0)	UG1-2	1.5	100	14.4 (500× 80.0)
2	UG2-1	2.0	100	1.0 (333.3× 40.0)	UG2-2	2.0	100	6.5 (500× 80.0)
3	UG3-1	3.0	100	0.4 (333.3× 40.0)	UG3-2	3.0	100	2.5 (500× 80.0)
4	UG4-1	2.0	150	1.6 (333.3× 30.0)	UG4-2	2.0	150	14.6 (500× 80.0)
5	UG5-1	3.0	150	0.6 (333.3× 30.0)	UG5-2	3.0	150	5.7 (500× 80.0)
6	UG6-1	4.0	150	0.3 (333.3× 30.0)	UG6-2	4.0	150	3.1 (500× 80.0)

Figs. 5 and 6 plot the shear stresses with the maximum out-of-plane deflections, *u*, in the webs and the web-flange junctions. The dotted lines in each plot denote the critical elastic buckling stresses obtained from the eigenvalue analyses.

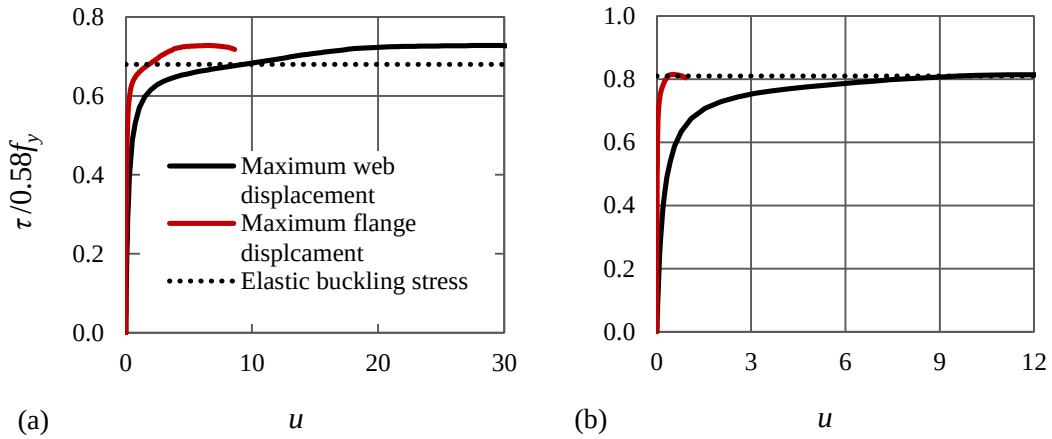

Figure 5*:* Load deflection plots for the out-of-plane displacements in flanges and webs for the unstiffened I-girders (a) UG2-1 (b) UG2-2

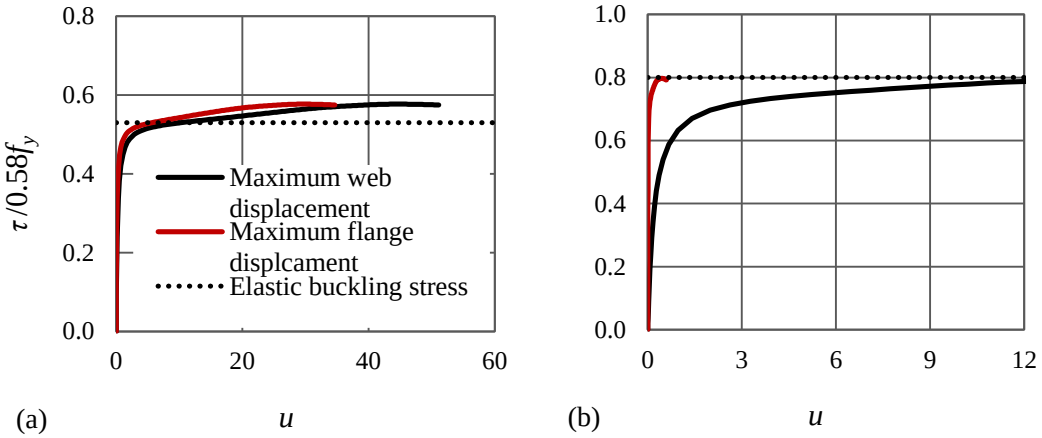

Figure 6: Load deflection plots for the out-of-plane displacements in flanges and webs for the unstiffened I-girders (a) UG3-1 (b) UG3-2

The following are gleaned from Figs. 5 and 6:

1. Figs. 5(a) and 5(b) show that the displacements are significant at the web-flange junctions for specimen UG2-1 (~20% of the web deflection at the peak load), whereas the displacement at the web-flange junction in specimen UG2-2 is less than 4% of the web out-of-plane displacement at the peak load. The flange moment of inertia in UG2-2 is nine times that of UG-1, and the cross-sectional area of the flange is four times that of UG2-1.

2. Similarly, from Figs. 6(a) and 6(b), a more significant deflection at the web-flange junction is observed for specimen UG3-1 than UG3-2, approximately 55% of the web deflection at the peak load. With an increase in the flange moment of inertia, the deflection at the web-flange junction reduces significantly to only 2% of that of the web deflection.

3. Figs. 5 and 6 show that using flanges with moments of inertia more than twice $I_{\min,f}$ reduces the deflection at the web boundaries. Consequently, the shear buckling strengths increase by 8% and 20%, respectively.

The maximum out-of-plane deflections at the web-flange junctions, relative to that of the web, for the 6 case studies or the 12 I-girders listed in Table 3 is illustrated in Fig. 7. The bar chart presents a comparison of the relative deflections obtained via elastic buckling analyses at the critical loads and the relative deflections in the nonlinear analyses at loads corresponding to elastic buckling, and at the peak loads from the nonlinear analyses.

The out-of-plane deflections at the web-flange junctions are less than 10% of the web displacements in I-girders that meet the flange moment of inertia criteria recommended in Section 3.2. Fig. 7 demonstrates that I-girders with flexible flanges can exhibit significant displacements at the web boundaries. At ultimate loads, the relative displacements at the web-flange junction exceed 50% of the relative displacement observed at the theoretical elastic critical buckling load for some cases (UG4-1, UG4-2, UG5-1, UG6-1, and UG6-2). This increase in relative displacements at the web-flange junctions at the ultimate loads is observed in unstiffened I-girders with greater post-buckling stress, i.e., girders with larger web slenderness ratios.

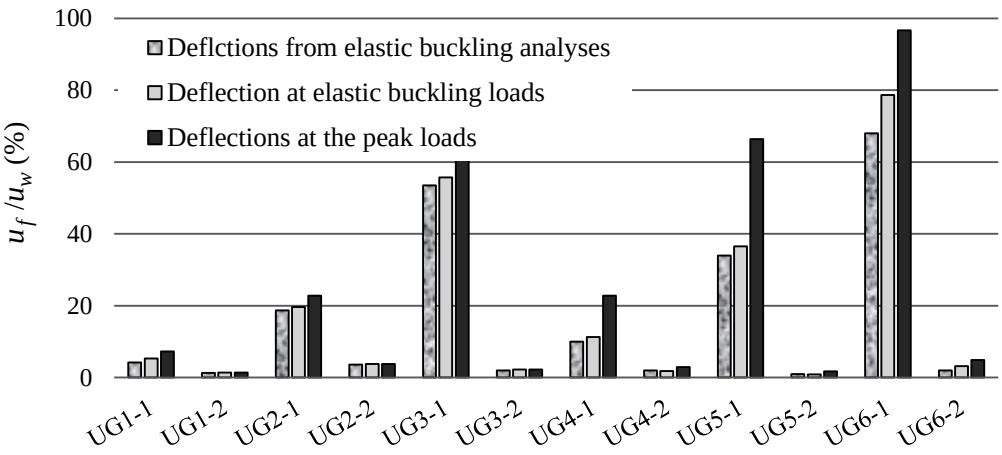

Figure 7: Comparison of the deflections for the seven case studies

The nonlinear analyses with insignificant imperfections yield results comparable to those from elastic buckling analyses at identical load levels. It is further noted that while the above comparisons are for nonlinear analyses with near-zero initial geometric imperfections, the out-of-plane displacements are more significant when more realistic values of initial imperfections are considered in the models, making the findings more concerning in practical design.

5. Conclusions

This paper offers new insights into the complex behavior of I-girders with flexible transverse stiffeners and flanges. This study questions established design assumptions regarding the boundary conditions of I-girder webs when estimating elastic shear buckling capacities. By examining modal deflections at the web boundaries through elastic shear buckling analyses, limitations on transverse stiffener and flange dimensions are suggested. The recommendations based on modal displacements are subsequently validated through a few nonlinear analyses.

The key findings in this paper are summarized below:

1. The transverse stiffeners satisfying the minimum moment of inertia specified in the design codes fail to restrict the deflection to a near zero value at the web-stiffener junction for smaller web aspect ratios. The maximum displacement at the web-stiffener junction is observed to be 22% of the maximum web displacement for an aspect ratio of 0.5.

2. Flanges that meet the minimum Specification requirements for flange width and thickness experience out-of-plane displacements at the web-flange junction, occasionally reaching levels comparable to the maximum displacement in the web. Such significant flange displacements are accompanied by web buckling stresses far below those of simply-supported web plates, particularly for panel aspect ratios ≥ 1.5. This is a cause for concern, considering that the shear strengths of I-sections are calculated as an algebraic sum of the elastic buckling and the postbucking stresses. This also poses interesting questions on the actual postbuckling mechanics of such I-sections.

3. From the nonlinear analyses, it is noted that for unstiffened I-girders with flexible flanges exhibiting substantial shear post-buckling, the relative displacement in the flanges at the ultimate load surpasses that estimated at the elastic buckling load. Nevertheless, it is demonstrated that by employing $I_f \geq 2I_{\min,f}$ ($I_{\min,f}$ is recommended in this paper by inverting the web height and length terms in the requirements for transverse stiffeners), the out-of-plane displacement at the web-flange junction can be limited to a value lower than 10% of the web's out-of-plane displacement at the peak load.

4. Based on these studies, the authors recommend using transverse stiffeners that satisfy $Is \geq 2I_{\min,s}$. Similarly, the flanges satisfying the limit $I_f \geq 2I_{\min,f}$ in addition to existing criteria, help achieve at least simply-supported boundary condition for the I-girder webs subjected to shear. These requirements also ensure minimal out-of-plane displacements at the stiffener and flange edges.

Acknowledgments
This research work received support from the Science and Engineering Research Board of India.

References

AASHTO (2020). *AASHTO LRFD bridge design specifications*, 9th Ed. American Association of State and Highway Transportation Officials, Washington, D.C.

ABAQUS. (2022). *[Computer Software]. Dassault systémes, Waltham, MA.*

AISC. (2022). *Specifications for structural steel buildings, ANSI/AISC 360-22*. American Institute of Steel Construction, Chicago, IL.

Al-azzawi, Z., Stratford, T., Rotter, J. M., Bisby, L.A. (2015). "Effect of flange and stiffener rigidity on the boundary conditions and shear buckling stress of plate girders." *Proceedings of 16th European Bridge Engineering Conference*. Edinburgh, Scotland.

Basler, K. (1961). *Strength of plate girders in shear*. Proc. ASCE; 87; (ST7), (October 1961); Reprint No. 186 (61-13). Vol. 185. Fritz Laboratory Reports.

Bleich, F. (1952). *Buckling strength of metal structures*. Mc Graw-Hill Book Company, Inc., Cardnr. 51-12588.

EN 1993-1-5. (2006). *Eurocode 3: Design of steel structures - Part 1-5: General rules - plated structural elements*. [Authority: The European Union Per Regulation 305/2011, Directive 98/34/EC, Directive 2004/18/EC].

Höglund, T. (1971). *Behaviour and strength of the web of thin plate I-girders*. Bulletin No.93 of the division of building statics and structural engineering. The Royal Institute of Technology, Stockholm, Sweden.

Höglund, T. (1997). "Shear buckling resistance of steel and aluminium plate girders." Thin-Walled Structures 29(1–4):13–30. doi: 10.1016/s0263-8231(97)00012-8.

Kim, Y. D. (2004). *Transverse stiffener requirements in straight and horizontally curved steel I-girders*. MS Thesis, Georgia Institute of Technology, Atlanta, GA.

Lapira, L., Gardner, L., Wadee, M.A. (2023). "Elastic local buckling formulae for thin-walled I-sections subjected to shear and direct stresses." *Thin-Walled Structures* 182:110150. doi: 10.1016/j.tws.2022.110150.

Lee, S. C., Davidson, J.S., Yoo, C. H. (1996). "Shear buckling coefficients of plate girder web panels." *Computers and Structures* 59(5):789–95. doi: 10.1016/0045-7949(95)00325-8.

Lee, S. C., Yoo, C.H., Yoon, D.Y. (2003). "New design rule for intermediate transverse stiffeners attached on web panels." *Journal of Structural Engineering* 129(12):1607–14. doi: 10.1061/(asce)0733-9445(2003)129:12(1607).

Nayak, N., Mariappan, A.S., Subramanian, L. (2021). "Improved characterization of elastic flexural and shear buckling strengths of I-sections." *Proceedings of the Annual Stability Conference Structural Stability Research Council, SSRC 2021*. Louisville, Kentucky.

Nayak, N, Subramanian, L. (2023). "Residual stresses: measurements and their influence on the ultimate shear strength of hybrid I-sections." *Proceedings of the 13th Structural Engineering Convention*. VNIT, Nagpur.

Pham, C. H., Hancock, G. J. (2009). "Shear buckling of thin-walled channel sections." *Journal of Constructional Steel Research* 65(3):578–85. doi: 10.1016/j.jcsr.2008.05.015.

Stein, M., Fralich, R. W. (1949). *Critical Shear stress of infinitely long, simply supported plate with transverse stiffeners*. NACA Tech Note 1851.

Subramanian, L., White, D. W. (2017a). "Flexural resistance of longitudinally stiffened I-girders. I: yield limit state." *Journal of Bridge Engineering* 22(1):04016099. doi: 10.1061/(asce)be.1943-5592.0000975.

Subramanian, L., White, D. W. (2017b). "Reassessment of the lateral torsional buckling resistance of rolled I-section members: moment gradient tests." *Journal of Structural Engineering* 143(4):04016203. doi: 10.1061/(asce)st.1943-541x.0001687.

Timoshenko, S. P. (1936). *Theory of elastic stability*. 1st ed. New York: McGraw- Hill.

Ziemian, R. D. (2010). *Guide to stability design criteria for metal structures*. 6th ed. John Wiley & Sons.